

EWSBS phenomenology in diphoton events

Presented by
Rafael L. Delgado

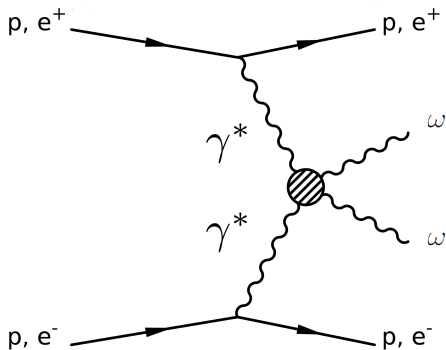


Antonio Dobado González, Felipe J. Llanes-Estrada,
Ivan León Merino, Miguel Espada Ruiz

Higgs Effective Field Theory 2018 (HEPFT 2018), Mainz, Germany

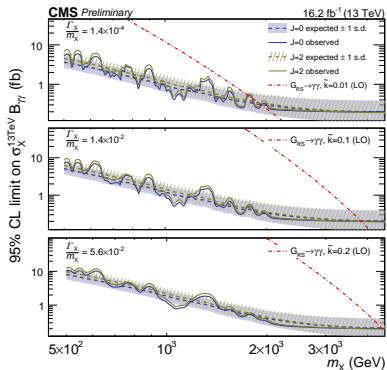
arXiv:1710.07548 [hep-ph], EPJC**77** no.4, 205; JHEP**07** 149; JHEP**02** 121;
J.Phys.G:Nucl.Part.Phys.**41** 025002.

Considered processes



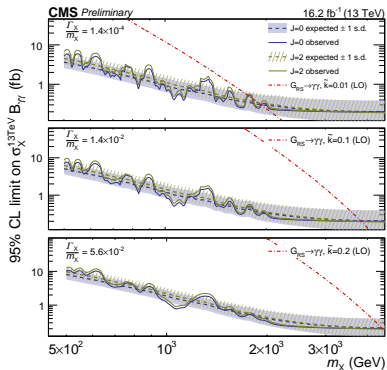
$$e^+e^- \rightarrow e^+e^- \gamma^* \gamma^*, \quad pp \rightarrow pp \gamma^* \gamma^*$$
$$\gamma^* \gamma^* \rightarrow (\text{EWSBS})$$

Empirical situation and motivation: $\gamma\gamma$ physics



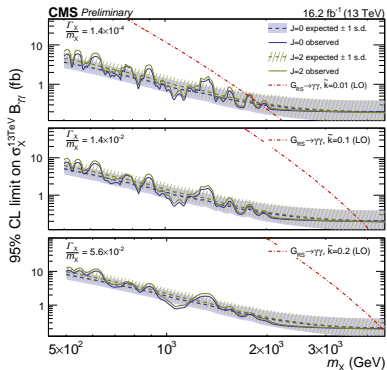
- Resonances in $\gamma\gamma$ channel, easy to detect (H, π_0, η, \dots).
- False alarm at the LHC!!
CMS-PAS-EXO-16-027, presented on ICHEP2016.
- According to CMS data, the diphoton excess (2.9σ) at $m_\chi \approx 750$ GeV is reduced to about 0.8σ .
- A resonance at $m_\chi \approx 750$ GeV in $\gamma\gamma$ without a counterpart in $V_L V_L \rightarrow V_L V_L$, problematic for strongly interacting models.
- Anyway, in this presentation, we will focus in $\gamma\gamma$.

Empirical situation and motivation: $\gamma\gamma$ physics



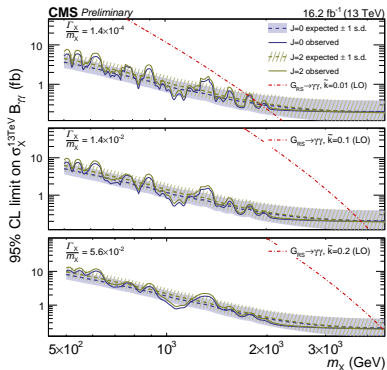
- Resonances in $\gamma\gamma$ channel, easy to detect (H, π_0, η, \dots).
- False alarm at the LHC!!
CMS-PAS-EXO-16-027, presented on ICHEP2016.
- According to CMS data, the diphoton excess (2.9σ) at $m_\chi \approx 750$ GeV is reduced to about 0.8σ .
- A resonance at $m_\chi \approx 750$ GeV in $\gamma\gamma$ without a counterpart in $V_L V_L \rightarrow V_L V_L$, problematic for strongly interacting models.
- Anyway, in this presentation, we will focus in $\gamma\gamma$.

Empirical situation and motivation: $\gamma\gamma$ physics



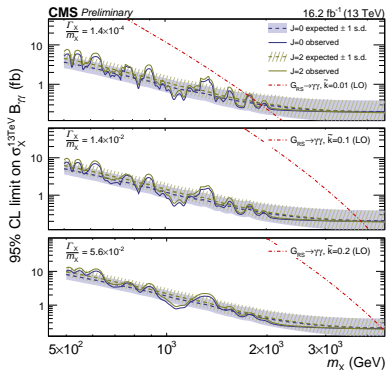
- Resonances in $\gamma\gamma$ channel, easy to detect (H, π_0, η, \dots).
- False alarm at the LHC!!
CMS-PAS-EXO-16-027, presented on ICHEP2016.
- According to CMS data, the diphoton excess (2.9σ) at $m_\chi \approx 750$ GeV is reduced to about 0.8σ .
- A resonance at $m_\chi \approx 750$ GeV in $\gamma\gamma$ without a counterpart in $V_L V_L \rightarrow V_L V_L$, problematic for strongly interacting models.
- Anyway, in this presentation, we will focus in $\gamma\gamma$.

Empirical situation and motivation: $\gamma\gamma$ physics



- Resonances in $\gamma\gamma$ channel, easy to detect (H, π_0, η, \dots).
- False alarm at the LHC!!
CMS-PAS-EXO-16-027, presented on ICHEP2016.
- According to CMS data, the diphoton excess (2.9σ) at $m_{\chi} \approx 750$ GeV is reduced to about 0.8σ .
- A resonance at $m_{\chi} \approx 750$ GeV in $\gamma\gamma$ without a counterpart in $V_L V_L \rightarrow V_L V_L$, problematic for strongly interacting models.
- Anyway, in this presentation, we will focus in $\gamma\gamma$.

Empirical situation and motivation: $\gamma\gamma$ physics



- Resonances in $\gamma\gamma$ channel, easy to detect (H, π_0, η, \dots).
- False alarm at the LHC!!
CMS-PAS-EXO-16-027, presented on ICHEP2016.
- According to CMS data, the diphoton excess (2.9σ) at $m_\chi \approx 750$ GeV is reduced to about 0.8σ .
- A resonance at $m_\chi \approx 750$ GeV in $\gamma\gamma$ without a counterpart in $V_L V_L \rightarrow V_L V_L$, problematic for strongly interacting models.
- Anyway, in this presentation, we will focus in $\gamma\gamma$.



CERN-EP-2018-014
2018/03/14

CMS-PPS-17-001
TOTEM 2018-001

Observation of proton-tagged, central (semi)exclusive production of high-mass lepton pairs in pp collisions at 13 TeV with the CMS–TOTEM precision proton spectrometer

The CMS and TOTEM Collaborations*

Abstract

The process $pp \rightarrow p\ell^+\ell^-p^{(*)}$, with $\ell^+\ell^-$ a muon or an electron pair produced at midrapidity with mass larger than 110 GeV, has been observed for the first time at the LHC in pp collisions at $\sqrt{s} = 13$ TeV. One of the two scattered protons is measured in the CMS-TOTEM precision proton spectrometer (CT-PPS), which operated for the first time in 2016. The second proton either remains intact or is excited and then dissociates into a low-mass state p^* , which is undetected. The measurement is based on an integrated luminosity of 9.4 fb^{-1} collected during standard, high-luminosity LHC operation. A total of 12 $\mu^+\mu^-$ and 8 e^+e^- pairs with $m(\ell^+\ell^-) > 110 \text{ GeV}$, and matching forward proton kinematics, are observed, with expected backgrounds of 1.49 ± 0.07 (stat) ± 0.53 (syst) and 2.36 ± 0.09 (stat) ± 0.47 (syst), respectively. This corresponds to an excess of more than five standard deviations over the expected background. The present result constitutes the first observation of proton-tagged $\gamma\gamma$ collisions at the electroweak scale. This measurement also demonstrates that CT-PPS performs according to the design specifications.

Empirical situation: $\gamma\gamma$ physics

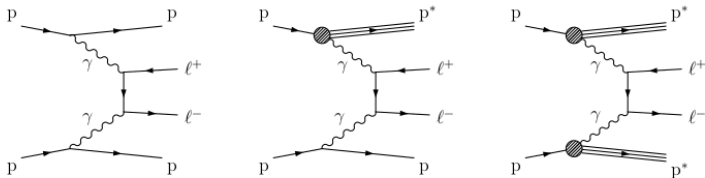


Figure 1: Production of lepton pairs by $\gamma\gamma$ fusion. The exclusive (left), single proton dissociation or semiexclusive (middle), and double proton dissociation (right) topologies are shown. The left and middle processes result in at least one intact final-state proton, and are considered signal in this analysis. The rightmost diagram is considered to be a background process.

Measurements of $\gamma\gamma \rightarrow$ Higgs and $\gamma\gamma \rightarrow W^+W^-$
in e^+e^- collisions at the Future Circular Collider

DAVID D'ENTERRIA¹

CERN, EP Department 1211 Geneva, Switzerland

PATRICIA REBELLO TELES²

Centro Brasileiro de Pesquisas Físicas - CBPF, 22290-180 Rio de Janeiro, Brazil

DANIEL E. MARTINS³

Universidade Federal do Rio de Janeiro - UFRJ, 21941-901 Rio de Janeiro, Brazil

arXiv:1712.07023v1 [hep-ph] 19 Dec 2017

Empirical situation: $\gamma\gamma$ physics

The measurements of the two-photon production of the Higgs boson and of W^\pm boson pairs in e^+e^- collisions at the Future Circular Collider (FCC-ee) are investigated. The processes $e^+e^- \xrightarrow{\gamma\gamma} e^+ H e^-, e^+ W^+ W^- e^-$ are computed using the effective photon approximation for electron-positron beams, and studied in their $H \rightarrow b\bar{b}$ and $W^+W^- \rightarrow 4j$ decay final-states including parton showering and hadronization, jet reconstruction, e^\pm forward tagging, and realistic experimental cuts. After selection criteria, up to 75 Higgs bosons and 6600 W^\pm pairs will be reconstructed on top of controllable continuum backgrounds at $\sqrt{s} = 240$ and 350 GeV for the total expected integrated luminosities, by tagging the scattered e^\pm with near-beam detectors. A 5σ observation of $\gamma\gamma \rightarrow H$ is thereby warranted, as well as high-statistics studies of triple γWW and quartic $\gamma\gamma WW$ electroweak couplings, improving by at least factors of 2 and 10 the current limits on dimension-6 anomalous quartic gauge couplings.

Empirical situation: $\gamma\gamma$ physics

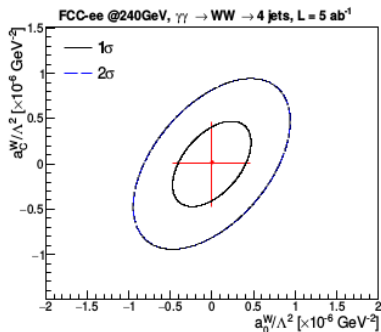


Figure 4: Expected 1σ and 2σ limits for the anomalous quartic gauge coupling parameters a_0^W/Λ and a_c^W/Λ , from the $e^+e^- \rightarrow \gamma\gamma \rightarrow W^+W^-(4j)$ measurement at $\sqrt{s} = 240 \text{ GeV}$ (FCC-ee, $\mathcal{L}_{\text{int}} = 5 \text{ ab}^{-1}$).

Studied framework

- We consider a strongly interacting EWSBS (Electroweak Chiral Lagrangian), in contrast to the weakly interacting one of the SM [PRL**114** 221803, PRD**91** 075017].
- We study the processes $VV \rightarrow VV$, $VV \rightarrow hh$ and $hh \rightarrow hh$, and extend the result to include $\gamma\gamma$ states [JHEP**07** 149].
- In order to minimize our assumptions over the (hypothetical) underlying theory, we will
 - use dispersion relations over a partial wave decomposition (the so-called unitarization procedures);
 - extend these unitarization procedures to the coupled-channels case [EPJC**77** no.4, 205];
 - and consider an Effective Field Theory, computed at the NLO level (within the limits of the Equivalence Theorem), with three would-be Goldstone bosons w and a Higgs-like boson h .
- The Effective Photon Approximation is used for approximating the generation of 2 hard γ 's from the initial pp and e^+e^- states [arXiv:1710.07548 [hep-ph]].

Studied framework

- We consider a strongly interacting EWSBS (Electroweak Chiral Lagrangian), in contrast to the weakly interacting one of the SM [PRL**114** 221803, PRD**91** 075017].
- We study the processes $VV \rightarrow VV$, $VV \rightarrow hh$ and $hh \rightarrow hh$, and extend the result to include $\gamma\gamma$ states [JHEP**07** 149].
- In order to minimize our assumptions over the (hypothetical) underlying theory, we will
 - use dispersion relations over a partial wave decomposition (the so-called unitarization procedures);
 - extend these unitarization procedures to the coupled-channels case [EPJC**77** no.4, 205];
 - and consider an Effective Field Theory, computed at the NLO level (within the limits of the Equivalence Theorem), with three would-be Goldstone bosons w and a Higgs-like boson h .
- The Effective Photon Approximation is used for approximating the generation of 2 hard γ 's from the initial pp and e^+e^- states [arXiv:1710.07548 [hep-ph]].

Studied framework

- We consider a strongly interacting EWSBS (Electroweak Chiral Lagrangian), in contrast to the weakly interacting one of the SM [PRL**114** 221803, PRD**91** 075017].
- We study the processes $VV \rightarrow VV$, $VV \rightarrow hh$ and $hh \rightarrow hh$, and extend the result to include $\gamma\gamma$ states [JHEP**07** 149].
- In order to minimize our assumptions over the (hypothetical) underlying theory, we will
 - use dispersion relations over a partial wave decomposition (the so-called unitarization procedures);
 - extend these unitarization procedures to the coupled-channels case [EPJC**77** no.4, 205];
 - and consider an Effective Field Theory, computed at the NLO level (within the limits of the Equivalence Theorem), with three would-be Goldstone bosons ω and a Higgs-like boson h .
- The Effective Photon Approximation is used for approximating the generation of 2 hard γ 's from the initial pp and e^+e^- states [arXiv:1710.07548 [hep-ph]].

Studied framework

- We consider a strongly interacting EWSBS (Electroweak Chiral Lagrangian), in contrast to the weakly interacting one of the SM [PRL**114** 221803, PRD**91** 075017].
- We study the processes $VV \rightarrow VV$, $VV \rightarrow hh$ and $hh \rightarrow hh$, and extend the result to include $\gamma\gamma$ states [JHEP**07** 149].
- In order to minimize our assumptions over the (hypothetical) underlying theory, we will
 - use dispersion relations over a partial wave decomposition (the so-called unitarization procedures);
 - extend these unitarization procedures to the coupled-channels case [EPJC**77** no.4, 205];
 - and consider an Effective Field Theory, computed at the NLO level (within the limits of the Equivalence Theorem), with three would-be Goldstone bosons ω and a Higgs-like boson h .
- The Effective Photon Approximation is used for approximating the generation of 2 hard γ 's from the initial pp and e^+e^- states [arXiv:1710.07548 [hep-ph]].

Studied framework

- We consider a strongly interacting EWSBS (Electroweak Chiral Lagrangian), in contrast to the weakly interacting one of the SM [PRL**114** 221803, PRD**91** 075017].
- We study the processes $VV \rightarrow VV$, $VV \rightarrow hh$ and $hh \rightarrow hh$, and extend the result to include $\gamma\gamma$ states [JHEP**07** 149].
- In order to minimize our assumptions over the (hypothetical) underlying theory, we will
 - use dispersion relations over a partial wave decomposition (the so-called unitarization procedures);
 - extend these unitarization procedures to the coupled-channels case [EPJC**77** no.4, 205];
 - and consider an Effective Field Theory, computed at the NLO level (within the limits of the Equivalence Theorem), with three would-be Goldstone bosons ω and a Higgs-like boson h .
- The Effective Photon Approximation is used for approximating the generation of 2 hard γ 's from the initial pp and e^+e^- states [arXiv:1710.07548 [hep-ph]].

Studied framework

- We consider a strongly interacting EWSBS (Electroweak Chiral Lagrangian), in contrast to the weakly interacting one of the SM [PRL**114** 221803, PRD**91** 075017].
- We study the processes $VV \rightarrow VV$, $VV \rightarrow hh$ and $hh \rightarrow hh$, and extend the result to include $\gamma\gamma$ states [JHEP**07** 149].
- In order to minimize our assumptions over the (hypothetical) underlying theory, we will
 - use dispersion relations over a partial wave decomposition (the so-called unitarization procedures);
 - extend these unitarization procedures to the coupled-channels case [EPJC**77** no.4, 205];
 - and consider an Effective Field Theory, computed at the NLO level (within the limits of the Equivalence Theorem), with three would-be Goldstone bosons ω and a Higgs-like boson h .
- The Effective Photon Approximation is used for approximating the generation of 2 hard γ 's from the initial pp and e^+e^- states [arXiv:1710.07548 [hep-ph]].

Studied framework

- We consider a strongly interacting EWSBS (Electroweak Chiral Lagrangian), in contrast to the weakly interacting one of the SM [PRL**114** 221803, PRD**91** 075017].
- We study the processes $VV \rightarrow VV$, $VV \rightarrow hh$ and $hh \rightarrow hh$, and extend the result to include $\gamma\gamma$ states [JHEP**07** 149].
- In order to minimize our assumptions over the (hypothetical) underlying theory, we will
 - use dispersion relations over a partial wave decomposition (the so-called unitarization procedures);
 - extend these unitarization procedures to the coupled-channels case [EPJC**77** no.4, 205];
 - and consider an Effective Field Theory, computed at the NLO level (within the limits of the Equivalence Theorem), with three would-be Goldstone bosons ω and a Higgs-like boson h .
- The Effective Photon Approximation is used for approximating the generation of 2 hard γ 's from the initial pp and e^+e^- states [arXiv:1710.07548 [hep-ph]].

Non-linear Electroweak Chiral Lagrangian

We have no clue of what, how or if new physics...

Non-linear EFT¹ for VV scattering at NLO level, minimally coupled to hh ,

$$\mathcal{L} = \frac{v^2}{4} g(h/f) \text{Tr}[(D_\mu U)^\dagger D^\mu U] + \frac{1}{2} \partial_\mu h \partial^\mu h - V(h),$$

where

$$g(h/v) = 1 + 2a \frac{h}{v} + b \left(\frac{h}{v}\right)^2 + \dots$$

$$V(h) = V_0 + \frac{M_h^2}{2} h^2 + \sum_{n=3}^{\infty} \lambda_n h^n$$

$$D_\mu U = \partial_\mu U + i\hat{W}_\mu U - iU\hat{B}_\mu.$$

M_h and λ_n are subleading in chiral counting.

¹Yellow Report: *C.Grojean, A.Falkowski, M.Trott, B.Fuks, *G.Buchalla, T.Plehn, G.Isidori, K.Tackmann, L.Brenner,...; LHCHSWG-DRAFT-INT-2016-002

Non-linear Electroweak Chiral Lagrangian

We have no clue of what, how or if new physics...

Non-linear EFT¹ for VV scattering at NLO level, minimally coupled to hh ,

$$\mathcal{L} = \frac{v^2}{4} g(h/f) \text{Tr}[(D_\mu U)^\dagger D^\mu U] + \frac{1}{2} \partial_\mu h \partial^\mu h - V(h),$$

where

$$g(h/v) = 1 + 2a \frac{h}{v} + b \left(\frac{h}{v}\right)^2 + \dots$$

$$V(h) = V_0 + \frac{M_h^2}{2} h^2 + \sum_{n=3}^{\infty} \lambda_n h^n$$

$$D_\mu U = \partial_\mu U + i\hat{W}_\mu U - iU\hat{B}_\mu.$$

M_h and λ_n are subleading in chiral counting.

¹Yellow Report: *C.Grojean, A.Falkowski, M.Trott, B.Fuks, *G.Buchalla, T.Plehn, G.Isidori, K.Tackmann, L.Brenner,...; LHCHSWG-DRAFT-INT-2016-002

Non-linear Electroweak Chiral Lagrangian

We have no clue of what, how or if new physics...

Non-linear EFT¹ for VV scattering at NLO level, minimally coupled to hh ,

$$\mathcal{L} = \frac{v^2}{4} g(h/f) \text{Tr}[(D_\mu U)^\dagger D^\mu U] + \frac{1}{2} \partial_\mu h \partial^\mu h - V(h),$$

where

$$g(h/v) = 1 + 2a \frac{h}{v} + b \left(\frac{h}{v} \right)^2 + \dots$$

$$V(h) = V_0 + \frac{M_h^2}{2} h^2 + \sum_{n=3}^{\infty} \lambda_n h^n$$

$$D_\mu U = \partial_\mu U + i\hat{W}_\mu U - iU\hat{B}_\mu.$$

M_h and λ_n are subleading in chiral counting.

¹Yellow Report: *C.Grojean, A.Falkowski, M.Trott, B.Fuks, *G.Buchalla, T.Plehn, G.Isidori, K.Tackmann, L.Brenner,...; LHCHSWG-DRAFT-INT-2016-002

Extension to $\gamma\gamma$ states

The covariant derivative is defined as²

$$D_\mu U = \partial_\mu U + i\hat{W}_\mu U - iU\hat{B}_\mu.$$

The photon field A arises from the couplings with $\hat{W}_{\mu\nu}$ and $\hat{B}_{\mu\nu}$ through a rotation to the physical basis; an anomalous three-particle coupling may appear

$$-c_W \frac{h}{v} \hat{W}_{\mu\nu} \hat{W}^{\mu\nu} - c_B \frac{h}{v} \hat{B}_{\mu\nu} \hat{B}^{\mu\nu} = -\frac{c_\gamma}{2} \frac{h}{v} e^2 A_{\mu\nu} A^{\mu\nu}$$

The next additional NLO counterterms are needed,

$$\begin{aligned} \mathcal{L}_{4'} = & a_1 \text{Tr}(U\hat{B}_{\mu\nu}U^\dagger\hat{W}^{\mu\nu}) \\ & + ia_2 \text{Tr}(U\hat{B}_{\mu\nu}U^\dagger[V^\mu, V^\nu]) \\ & - ia_3 \text{Tr}(\hat{W}_{\mu\nu}[V^\mu, V^\nu]) \end{aligned}$$

²Work in collaboration with M.J.Herrero and J.J.Sanz-Cillero, [JHEP1407\(2014\)149](#).

Extension to $\gamma\gamma$ states

The covariant derivative is defined as²

$$D_\mu U = \partial_\mu U + i\hat{W}_\mu U - iU\hat{B}_\mu.$$

The photon field A arises from the couplings with $\hat{W}_{\mu\nu}$ and $\hat{B}_{\mu\nu}$ through a rotation to the physical basis; an anomalous three-particle coupling may appear

$$-c_W \frac{h}{v} \hat{W}_{\mu\nu} \hat{W}^{\mu\nu} - c_B \frac{h}{v} \hat{B}_{\mu\nu} \hat{B}^{\mu\nu} = -\frac{c_\gamma}{2} \frac{h}{v} e^2 A_{\mu\nu} A^{\mu\nu}$$

The next additional NLO counterterms are needed,

$$\begin{aligned} \mathcal{L}_{4'} = & a_1 \text{Tr}(U\hat{B}_{\mu\nu}U^\dagger\hat{W}^{\mu\nu}) \\ & + ia_2 \text{Tr}(U\hat{B}_{\mu\nu}U^\dagger[V^\mu, V^\nu]) \\ & - ia_3 \text{Tr}(\hat{W}_{\mu\nu}[V^\mu, V^\nu]) \end{aligned}$$

²Work in collaboration with M.J.Herrero and J.J.Sanz-Cillero, [JHEP1407\(2014\)149](#).

Extension to $\gamma\gamma$ states

The covariant derivative is defined as²

$$D_\mu U = \partial_\mu U + i\hat{W}_\mu U - iU\hat{B}_\mu.$$

The photon field A arises from the couplings with $\hat{W}_{\mu\nu}$ and $\hat{B}_{\mu\nu}$ through a rotation to the physical basis; an anomalous three-particle coupling may appear

$$-c_W \frac{h}{v} \hat{W}_{\mu\nu} \hat{W}^{\mu\nu} - c_B \frac{h}{v} \hat{B}_{\mu\nu} \hat{B}^{\mu\nu} = -\frac{c_\gamma}{2} \frac{h}{v} e^2 A_{\mu\nu} A^{\mu\nu}$$

The next additional NLO counterterms are needed,

$$\begin{aligned} \mathcal{L}_{4'} = & a_1 \text{Tr}(U\hat{B}_{\mu\nu}U^\dagger\hat{W}^{\mu\nu}) \\ & + ia_2 \text{Tr}(U\hat{B}_{\mu\nu}U^\dagger[V^\mu, V^\nu]) \\ & - ia_3 \text{Tr}(\hat{W}_{\mu\nu}[V^\mu, V^\nu]) \end{aligned}$$

²Work in collaboration with M.J.Herrero and J.J.Sanz-Cillero, [JHEP1407\(2014\)149](#).

Extension to $\gamma\gamma$ states

The covariant derivative is defined as²

$$D_\mu U = \partial_\mu U + i\hat{W}_\mu U - iU\hat{B}_\mu.$$

The photon field A arises from the couplings with $\hat{W}_{\mu\nu}$ and $\hat{B}_{\mu\nu}$ through a rotation to the physical basis; an anomalous three-particle coupling may appear

$$-c_W \frac{h}{v} \hat{W}_{\mu\nu} \hat{W}^{\mu\nu} - c_B \frac{h}{v} \hat{B}_{\mu\nu} \hat{B}^{\mu\nu} = -\frac{c_\gamma}{2} \frac{h}{v} e^2 A_{\mu\nu} A^{\mu\nu}$$

The next additional NLO counterterms are needed,

$$\begin{aligned} \mathcal{L}_{4'} = & a_1 \text{Tr}(U\hat{B}_{\mu\nu}U^\dagger\hat{W}^{\mu\nu}) \\ & + ia_2 \text{Tr}(U\hat{B}_{\mu\nu}U^\dagger[V^\mu, V^\nu]) \\ & - ia_3 \text{Tr}(\hat{W}_{\mu\nu}[V^\mu, V^\nu]) \end{aligned}$$

²Work in collaboration with M.J.Herrero and J.J.Sanz-Cillero, [JHEP1407\(2014\)149](#).

Extension to $\gamma\gamma$ states

The covariant derivative is defined as²

$$D_\mu U = \partial_\mu U + i\hat{W}_\mu U - iU\hat{B}_\mu.$$

The photon field A arises from the couplings with $\hat{W}_{\mu\nu}$ and $\hat{B}_{\mu\nu}$ through a rotation to the physical basis; an anomalous three-particle coupling may appear

$$-c_W \frac{h}{v} \hat{W}_{\mu\nu} \hat{W}^{\mu\nu} - c_B \frac{h}{v} \hat{B}_{\mu\nu} \hat{B}^{\mu\nu} = -\frac{c_\gamma}{2} \frac{h}{v} e^2 A_{\mu\nu} A^{\mu\nu}$$

The next additional NLO counterterms are needed,

$$\begin{aligned} \mathcal{L}_{4'} = & a_1 \text{Tr}(U\hat{B}_{\mu\nu}U^\dagger\hat{W}^{\mu\nu}) \\ & + ia_2 \text{Tr}(U\hat{B}_{\mu\nu}U^\dagger[V^\mu, V^\nu]) \\ & - ia_3 \text{Tr}(\hat{W}_{\mu\nu}[V^\mu, V^\nu]) \end{aligned}$$

²Work in collaboration with M.J.Herrero and J.J.Sanz-Cillero, [JHEP1407\(2014\)149](#).

Extension to $\gamma\gamma$ states

The covariant derivative is defined as²

$$D_\mu U = \partial_\mu U + i\hat{W}_\mu U - iU\hat{B}_\mu.$$

The photon field A arises from the couplings with $\hat{W}_{\mu\nu}$ and $\hat{B}_{\mu\nu}$ through a rotation to the physical basis; an anomalous three-particle coupling may appear

$$-c_W \frac{h}{v} \hat{W}_{\mu\nu} \hat{W}^{\mu\nu} - c_B \frac{h}{v} \hat{B}_{\mu\nu} \hat{B}^{\mu\nu} = -\frac{c_\gamma}{2} \frac{h}{v} e^2 A_{\mu\nu} A^{\mu\nu}$$

The next additional NLO counterterms are needed,

$$\begin{aligned} \mathcal{L}_{4'} = & a_1 \text{Tr}(U\hat{B}_{\mu\nu}U^\dagger\hat{W}^{\mu\nu}) \\ & + ia_2 \text{Tr}(U\hat{B}_{\mu\nu}U^\dagger[V^\mu, V^\nu]) \\ & - ia_3 \text{Tr}(\hat{W}_{\mu\nu}[V^\mu, V^\nu]) \end{aligned}$$

²Work in collaboration with M.J.Herrero and J.J.Sanz-Cillero, [JHEP1407\(2014\)149](#).

Current and future constraints on Higgs couplings in the nonlinear Effective Theory

Jorge de Blas,^{a,b} Otto Eberhardt,^c and Claudius Krause^{c,d}

^a*Dipartimento di Fisica e Astronomia "Galileo Galilei", Università di Padova, Via Marzolo 8, I-35131 Padova, Italy*

^b*INFN, Sezione di Padova, Via Marzolo 8, I-35131 Padova, Italy*

^c*IFIC, Universitat de Valencia-CSIC, Apt. Correus 22085, E-46071 Valencia, Spain*

^d*Theoretical Physics Department, Fermi National Accelerator Laboratory, Batavia, IL, 60510, USA*

E-mail: Jorge.DeBlasMateo@pd.infn.it, Otto.Eberhardt@ific.uv.es, Claudius.Krause@ific.uv.es

ABSTRACT: We perform a Bayesian statistical analysis of the constraints on the nonlinear Effective Theory given by the Higgs electroweak chiral Lagrangian. We obtain bounds on the effective coefficients entering in Higgs observables at the leading order, using all available Higgs-boson signal strengths from the LHC runs 1 and 2. Using a prior dependence study of the solutions, we discuss the results within the context of natural-sized Wilson coefficients. We further study the expected sensitivities to the different Wilson coefficients at various possible future colliders. Finally, we interpret our results in terms of some minimal composite Higgs models.

Experimental bounds

Parameter	Fit results		
	Full dataset	Run 1 only	Run 2 only
c_V	1.02 ± 0.06	$0.96^{+0.08}_{-0.09}$	1.09 ± 0.08
c_t	$0.96^{+0.12}_{-0.13}$	$1.16^{+0.32}_{-0.43}$	$0.93^{+0.13}_{-0.14}$
c_b	0.94 ± 0.14	$0.93^{+0.24}_{-0.22}$	$1.01^{+0.20}_{-0.18}$
c_c	1.04 ± 0.51	1.04 ± 0.51	1.03 ± 0.51
c_τ	1.03 ± 0.10	1.04 ± 0.15	1.06 ± 0.15
c_μ	$0.61^{+0.42}_{-0.40}$	$< 1.1 @ 68\%$ $(< 1.76 @ 95\%)$	$0.65^{+0.45}_{-0.43}$
c_g	$0.00^{+0.11}_{-0.09}$	$-0.12^{+0.35}_{-0.27}$	$0.04^{+0.12}_{-0.10}$
c_γ	0.06 ± 0.24	$-0.34^{+0.46}_{-0.37}$	0.26 ± 0.31
$c_{Z\gamma}$	0.00 ± 0.50	0.00 ± 0.50	0.00 ± 0.50

As it would require measuring the coupling of two Higgses, there is no experimental bound over the value of b parameter.

Collinear photon approximation: e^+e^- collider

- Aimed for the ICL perspectives (energy of ~ 1 TeV).
- Elastic scattering.

$$\frac{d\sigma(e^-e^+ \rightarrow e^-e^+\gamma\gamma \rightarrow e^-e^+\omega\omega)}{dsdp_T^2}(s_{\gamma\gamma}, \theta) = \frac{1}{s_{\gamma\gamma}} \int_{x_{min}}^{x_{max}} dx_1 \frac{f(x_1)}{x_1} f\left(\frac{s_{\gamma\gamma}}{s_{ee}x}\right) \frac{d\sigma_{\gamma\gamma \rightarrow \omega\omega}(s_{\gamma\gamma}, \theta)}{dp_T^2},$$

$$\frac{dn}{dx} = f(x) = \frac{\alpha}{\pi x} \int_{Q_{min}^2}^{Q_{max}^2} \left[\frac{Q^2 - Q_{min}^2}{Q^4} (1-x) + \frac{x^2}{2Q^2} \right] dQ^2.$$

Collinear photon approximation: e^+e^- collider

- Aimed for the ICL prospectives (energy of ~ 1 TeV).
- Elastic scattering.

$$\frac{d\sigma(e^-e^+ \rightarrow e^-e^+\gamma\gamma \rightarrow e^-e^+\omega\omega)}{dsdp_T^2}(s_{\gamma\gamma}, \theta) = \frac{1}{s_{\gamma\gamma}} \int_{x_{min}}^{x_{max}} dx_1 \frac{f(x_1)}{x_1} f\left(\frac{s_{\gamma\gamma}}{s_{ee}x}\right) \frac{d\sigma_{\gamma\gamma \rightarrow \omega\omega}(s_{\gamma\gamma}, \theta)}{dp_T^2},$$

$$\frac{dn}{dx} = f(x) = \frac{\alpha}{\pi x} \int_{Q_{min}^2}^{Q_{max}^2} \left[\frac{Q^2 - Q_{min}^2}{Q^4} (1-x) + \frac{x^2}{2Q^2} \right] dQ^2.$$

Collinear photon approximation: e^+e^- collider

- Aimed for the ICL prospectives (energy of ~ 1 TeV).
- Elastic scattering.

$$\frac{d\sigma(e^-e^+ \rightarrow e^-e^+\gamma\gamma \rightarrow e^-e^+\omega\omega)}{dsdp_T^2}(s_{\gamma\gamma}, \theta) = \frac{1}{s_{\gamma\gamma}} \int_{x_{min}}^{x_{max}} dx_1 \frac{f(x_1)}{x_1} f\left(\frac{s_{\gamma\gamma}}{s_{ee}x}\right) \frac{d\sigma_{\gamma\gamma \rightarrow \omega\omega}(s_{\gamma\gamma}, \theta)}{dp_T^2},$$

$$\frac{dn}{dx} = f(x) = \frac{\alpha}{\pi x} \int_{Q_{min}^2}^{Q_{max}^2} \left[\frac{Q^2 - Q_{min}^2}{Q^4} (1-x) + \frac{x^2}{2Q^2} \right] dQ^2.$$

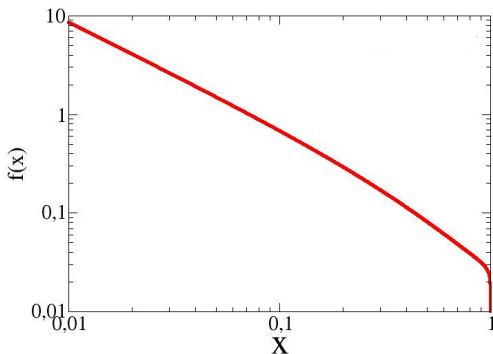
Collinear photon approximation: e^+e^- collider

- Aimed for the ICL prospectives (energy of ~ 1 TeV).
- Elastic scattering.

$$\frac{d\sigma(e^-e^+ \rightarrow e^-e^+\gamma\gamma \rightarrow e^-e^+\omega\omega)}{dsdp_T^2}(s_{\gamma\gamma}, \theta) = \frac{1}{s_{\gamma\gamma}} \int_{x_{min}}^{x_{max}} dx_1 \frac{f(x_1)}{x_1} f\left(\frac{s_{\gamma\gamma}}{s_{ee}x}\right) \frac{d\sigma_{\gamma\gamma \rightarrow \omega\omega}(s_{\gamma\gamma}, \theta)}{dp_T^2},$$

$$\frac{dn}{dx} = f(x) = \frac{\alpha}{\pi x} \int_{Q_{min}^2}^{Q_{max}^2} \left[\frac{Q^2 - Q_{min}^2}{Q^4} (1-x) + \frac{x^2}{2Q^2} \right] dQ^2.$$

Collinear photon approximation: pp collider



Photon number density per unit x (fractional energy taken from the electron). $s_{ee} = 1 \text{ TeV}^2$.

Collinear photon approximation: pp collider

- Elastic scattering: protons in the initial state remain unchanged. Elastic regime. Collinear photon flux in the proton and form factors are used here. CT-PPS (CMS-TOTEM) and AFP (ATLAS Forward Detector) aim at detecting elastically scattered protons near the beampipe.
- Deep Inelastic Scattering: protons are destroyed. Photons are partons of the protons (proper PDFs). CT14 and NNPDF are used here.
- Inelastic regime (not necessarily DIS): baryon resonance energy region. **Actually, we expect most of the cross section here.** We need to incorporate data from Jefferson laboratory and other mid-energy facilities. Convenient parametrization: LUX photon effective pdf [PRL117 no.24, 242002]. It integrates low- Q^2 data from A1, CLAS and Hermes GD11-P. The set LUXqed_plus_PDF4LHC15_nnlo_100 is used here.

Collinear photon approximation: pp collider

- Elastic scattering: protons in the initial state remain unchanged. Elastic regime. Collinear photon flux in the proton and form factors are used here. CT-PPS (CMS-TOTEM) and AFP (ATLAS Forward Detector) aim at detecting elastically scattered protons near the beampipe.
- Deep Inelastic Scattering: protons are destroyed. Photons are partons of the protons (proper PDFs). CT14 and NNPDF are used here.
- Inelastic regime (not necessarily DIS): baryon resonance energy region. **Actually, we expect most of the cross section here.** We need to incorporate data from Jefferson laboratory and other mid-energy facilities. Convenient parametrization: LUX photon effective pdf [PRL117 no.24, 242002]. It integrates low- Q^2 data from A1, CLAS and Hermes GD11-P. The set LUXqed_plus_PDF4LHC15_nnlo_100 is used here.

Collinear photon approximation: pp collider

- Elastic scattering: protons in the initial state remain unchanged. Elastic regime. Collinear photon flux in the proton and form factors are used here. CT-PPS (CMS-TOTEM) and AFP (ATLAS Forward Detector) aim at detecting elastically scattered protons near the beampipe.
- Deep Inelastic Scattering: protons are destroyed. Photons are partons of the protons (proper PDFs). CT14 and NNPDF are used here.
- Inelastic regime (not necessarily DIS): baryon resonance energy region. **Actually, we expect most of the cross section here.** We need to incorporate data from Jefferson laboratory and other mid-energy facilities. Convenient parametrization: LUX photon *effective pdf* [PRL117 no.24, 242002]. It integrates low- Q^2 data from A1, CLAS and Hermes GD11-P. The set LUXqed_plus_PDF4LHC15_nnlo_100 is used here.

Collinear photon approximation: pp collider

- Elastic scattering: protons in the initial state remain unchanged. Elastic regime. Collinear photon flux in the proton and form factors are used here. CT-PPS (CMS-TOTEM) and AFP (ATLAS Forward Detector) aim at detecting elastically scattered protons near the beampipe.
- Deep Inelastic Scattering: protons are destroyed. Photons are partons of the protons (proper PDFs). CT14 and NNPDF are used here.
- Inelastic regime (not necessarily DIS): baryon resonance energy region. **Actually, we expect most of the cross section here.** We need to incorporate data from Jefferson laboratory and other mid-energy facilities. Convenient parametrization: LUX photon *effective pdf* [PRL**117** no.24, 242002]. It integrates low- Q^2 data from A1, CLAS and Hermes GD11-P. The set LUXqed_plus_PDF4LHC15_nnlo_100 is used here.

$$\frac{d\sigma_{pp \rightarrow ppW^+W^-}}{ds_{\gamma\gamma}} = \int dx dy E_p^2 \frac{f(x)}{E_p x} \frac{f(y)}{E_p y} \sigma_{\gamma\gamma \rightarrow W_L^+ W_L^-} \delta(s_{\gamma\gamma} - 4xyE_p^2)$$

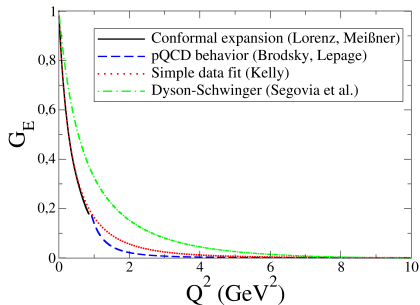
$$= \int dx \frac{1}{s_{\gamma\gamma}} \frac{f(x)}{x} f\left(\frac{s_{\gamma\gamma}}{4E_p^2 x}\right) \sigma_{\gamma\gamma \rightarrow W_L^+ W_L^-}$$

$$f(x) = \frac{\alpha}{\pi x} \int_{Q_{\min}^2}^{\infty} dQ^2 (1-x) \frac{Q^2 - Q_{\min}^2}{Q^4} D + \frac{x^2}{2Q^2} C$$

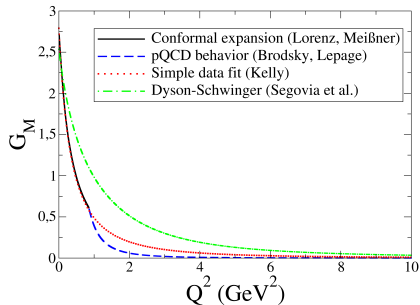
$$C = G_M^2, \quad D = \frac{4M_p^2 G_E^2 + Q^2 G_M^2}{4M_p^2 + Q^2}$$

$$Q_{\min}^2 = (M_p x)^2 / (1-x)$$

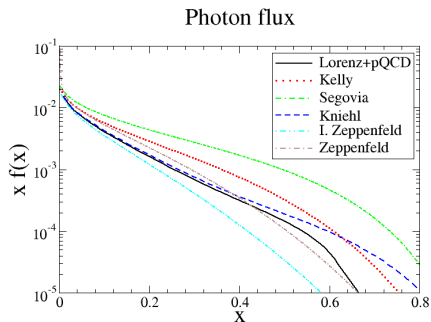
Sachs electric proton form factor



Sachs magnetic proton form factor

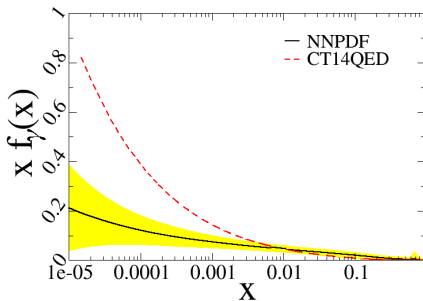
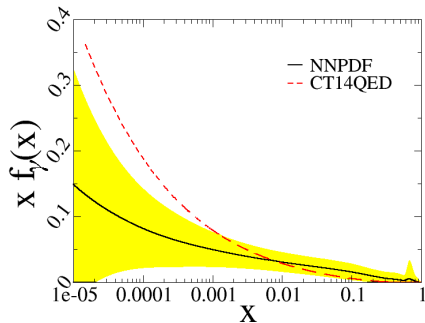


Some form factor parametrizations and theoretical computations as functions of Q^2 taken from the ample literature.



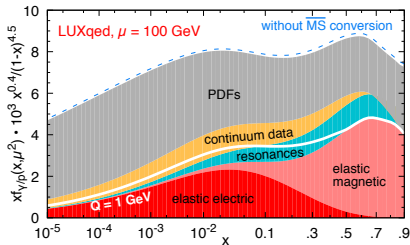
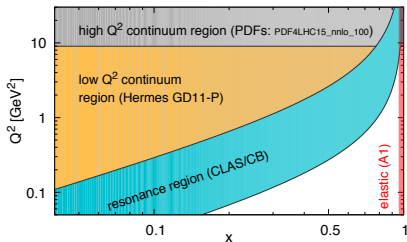
Photon flux. Continuous black line: parametrization matching dispersion relations at low momentum and counting rules at high Q^2 .

pp in the initial state, DIS



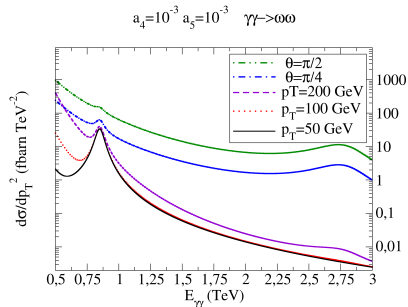
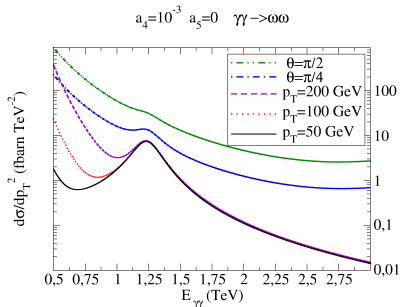
Product of the photon distribution function by x . Solid, black line: NNPDF extraction (with uncertainty as the shadowed yellow band). Dashed red line: CTQ14 set. The left plot takes $Q = 100 \text{ GeV}$, the right plot $Q = 1 \text{ TeV}$.

pp in the initial state, inelastic (not neces. DIS)

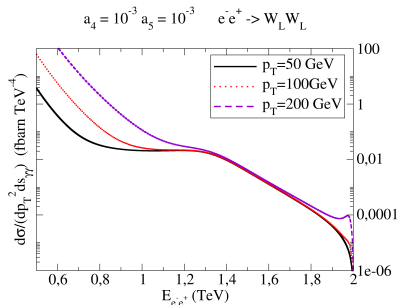
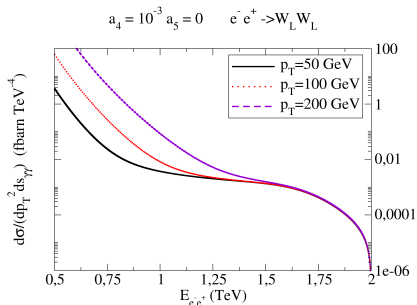


Figs. from [PRL**117** no.24, 242002], LUXqed. Left, scattering regime (white region, inaccessible at leading order in QED). Right: contribution to the photon *effective PDF* at $\mu = 100$ GeV, multiplied by $10^3 x^{0.4} / (1-x)^{4.5}$.

Base cases

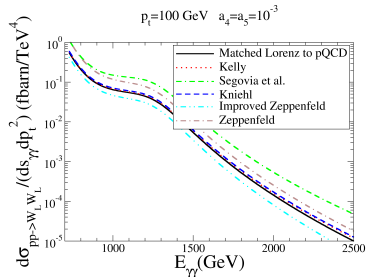
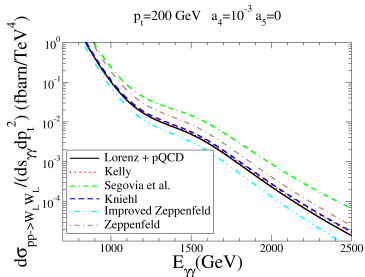
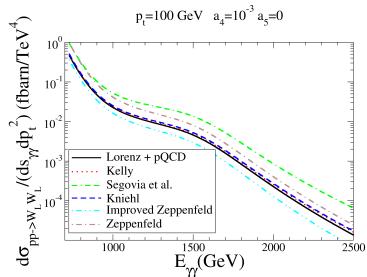
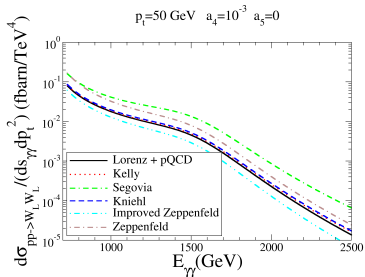


Differential cross section for $\gamma\gamma \rightarrow \omega\omega$. Left: $a_4 = 10^{-3}$, $a_5 = 0$. Right: $a_4 = a_5 = 10^{-3}$. Both sets introduce resonances around 1 TeV .

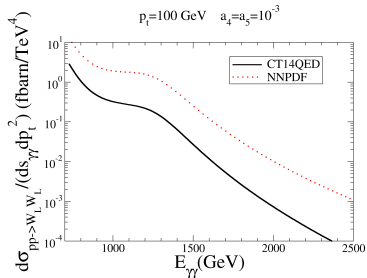
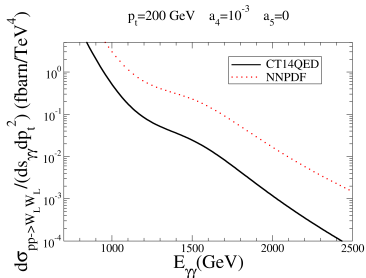
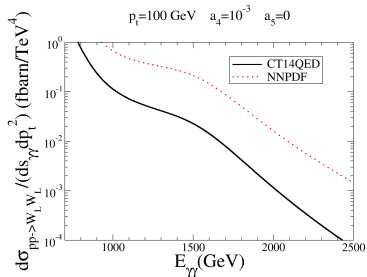
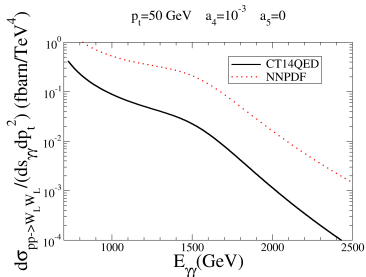


Differential cross sections from the previous slides, convoluted with the photon flux factors for a e^+e^- collider. The e^+e^- energy is fixed at 2 TeV.

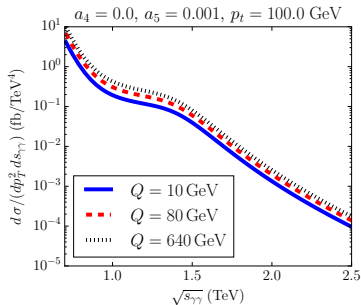
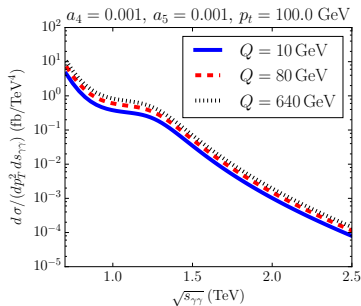
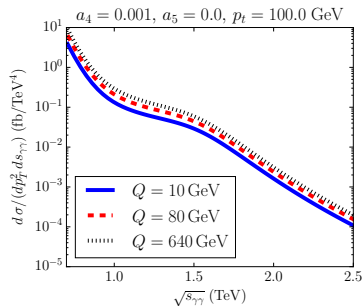
pp collider, elastic case



pp collider, DIS



pp collider, inelastic (not necess. DIS)



Conclusions: our work

- We have performed a comprehensive study of the unitarized amplitudes involving $\gamma\gamma$ in the initial state, and used the Effective Photon Approximation for collider phenomenology in pp and e^+e^- .
- While the cross sections are naturally small, as we have quantified, they are very clean if the outgoing elastically scattered protons can be tagged.
- Concerning the *elastic cross section*, the number of events to be found increases with p_t , **for modest values** thereof. If a new resonance was around $E_{\gamma\gamma} = 1$ TeV, σ would be rather flat in E and around 10^2 fbarn/TeV⁴.
- This means that an integrated luminosity of 300 fbarn⁻¹ at the LHC run-II would prove insufficient to gather enough events at this high invariant boson-boson mass.
- DIS (both protons dissociate): these events are difficult to isolate because the non-photon-initiated background is too large, leaving activity in the central silicon trackers.

Conclusions: our work

- We have performed a comprehensive study of the unitarized amplitudes involving $\gamma\gamma$ in the initial state, and used the Effective Photon Approximation for collider phenomenology in pp and e^+e^- .
- While the cross sections are naturally small, as we have quantified, they are very clean if the outgoing elastically scattered protons can be tagged.
- Concerning the *elastic cross section*, the number of events to be found increases with p_t , **for modest values** thereof. If a new resonance was around $E_{\gamma\gamma} = 1$ TeV, σ would be rather flat in E and around 10^2 fbarn/TeV⁴.
- This means that an integrated luminosity of 300 fbarn⁻¹ at the LHC run-II would prove insufficient to gather enough events at this high invariant boson-boson mass.
- DIS (both protons dissociate): these events are difficult to isolate because the non-photon-initiated background is too large, leaving activity in the central silicon trackers.

Conclusions: our work

- We have performed a comprehensive study of the unitarized amplitudes involving $\gamma\gamma$ in the initial state, and used the Effective Photon Approximation for collider phenomenology in pp and e^+e^- .
- While the cross sections are naturally small, as we have quantified, they are very clean if the outgoing elastically scattered protons can be tagged.
- Concerning the *elastic cross section*, the number of events to be found increases with p_t , **for modest values** thereof. If a new resonance was around $E_{\gamma\gamma} = 1 \text{ TeV}$, σ would be rather flat in E and around 10^2 fbarn/TeV^4 .
- This means that an integrated luminosity of 300 fbarn^{-1} at the LHC run-II would prove insufficient to gather enough events at this high invariant boson-boson mass.
- DIS (both protons dissociate): these events are difficult to isolate because the non-photon-initiated background is too large, leaving activity in the central silicon trackers.

Conclusions: our work

- We have performed a comprehensive study of the unitarized amplitudes involving $\gamma\gamma$ in the initial state, and used the Effective Photon Approximation for collider phenomenology in pp and e^+e^- .
- While the cross sections are naturally small, as we have quantified, they are very clean if the outgoing elastically scattered protons can be tagged.
- Concerning the *elastic cross section*, the number of events to be found increases with p_t , **for modest values** thereof. If a new resonance was around $E_{\gamma\gamma} = 1 \text{ TeV}$, σ would be rather flat in E and around 10^2 fbarn/TeV^4 .
- This means that an integrated luminosity of 300 fbarn^{-1} at the LHC run-II would prove insufficient to gather enough events at this high invariant boson-boson mass.
- DIS (both protons dissociate): these events are difficult to isolate because the non-photon-initiated background is too large, leaving activity in the central silicon trackers.

Conclusions: our work

- We have performed a comprehensive study of the unitarized amplitudes involving $\gamma\gamma$ in the initial state, and used the Effective Photon Approximation for collider phenomenology in pp and e^+e^- .
- While the cross sections are naturally small, as we have quantified, they are very clean if the outgoing elastically scattered protons can be tagged.
- Concerning the *elastic cross section*, the number of events to be found increases with p_t , **for modest values** thereof. If a new resonance was around $E_{\gamma\gamma} = 1 \text{ TeV}$, σ would be rather flat in E and around 10^2 fbarn/TeV^4 .
- This means that an integrated luminosity of 300 fbarn^{-1} at the LHC run-II would prove insufficient to gather enough events at this high invariant boson-boson mass.
- DIS (both protons dissociate): these events are difficult to isolate because the non-photon-initiated background is too large, leaving activity in the central silicon trackers.

Conclusions

- Resonance-mediated inelastic (but not deeply inelastic): the proton dissociates but mostly in the forward direction. More promising, but precise predictions are here difficult because we find quite some systematic difference due to the chosen pdf set; one can opt for the newest LUXQED set.
- Reson. below 1 TeV, the situation is a bit better. Cross sections, an order of magnitude larger.
- Reson. of higher masses: maybe in collisions involving heavy ions. Pb-Pb: enhanced by a factor $(Z = 82)^2$, lost to a factor 2000 smaller luminosity than in pp collisions with the current LHC; perhaps p-Pb is optimal.
- Proposed luminosity of the CLIC collider, $\sim 650 \text{ fbarn}^1/\text{yr}$; our resonance σ , 10^3 fbarn ; only a couple of events per year. While CLIC may be apt for exploring vector resonances that couple in an s-wave to e^+e^- , it will fall short in luminosity for scalar or tensor resonances in $\gamma\gamma$ physics.

Conclusions

- Resonance-mediated inelastic (but not deeply inelastic): the proton dissociates but mostly in the forward direction. More promising, but precise predictions are here difficult because we find quite some systematic difference due to the chosen pdf set; one can opt for the newest LUXQED set.
- Reson. below 1 TeV, the situation is a bit better. Cross sections, an order of magnitude larger.
- Reson. of higher masses: maybe in collisions involving heavy ions. Pb-Pb: enhanced by a factor $(Z = 82)^2$, lost to a factor 2000 smaller luminosity than in pp collisions with the current LHC; perhaps p-Pb is optimal.
- Proposed luminosity of the CLIC collider, $\sim 650 \text{ fbarn}^1/\text{yr}$; our resonance σ , 10^3 fbarn ; only a couple of events per year. While CLIC may be apt for exploring vector resonances that couple in an s-wave to e^+e^- , it will fall short in luminosity for scalar or tensor resonances in $\gamma\gamma$ physics.

Conclusions

- Resonance-mediated inelastic (but not deeply inelastic): the proton dissociates but mostly in the forward direction. More promising, but precise predictions are here difficult because we find quite some systematic difference due to the chosen pdf set; one can opt for the newest LUXQED set.
- Reson. below 1 TeV, the situation is a bit better. Cross sections, an order of magnitude larger.
- Reson. of higher masses: maybe in collisions involving heavy ions. Pb-Pb: enhanced by a factor $(Z = 82)^2$, lost to a factor 2000 smaller luminosity than in pp collisions with the current LHC; perhaps p-Pb is optimal.
- Proposed luminosity of the CLIC collider, $\sim 650 \text{ fbarn}^1/\text{yr}$; our resonance σ , 10^3 fbarn ; only a couple of events per year. While CLIC may be apt for exploring vector resonances that couple in an s-wave to e^+e^- , it will fall short in luminosity for scalar or tensor resonances in $\gamma\gamma$ physics.

Conclusions

- Resonance-mediated inelastic (but not deeply inelastic): the proton dissociates but mostly in the forward direction. More promising, but precise predictions are here difficult because we find quite some systematic difference due to the chosen pdf set; one can opt for the newest LUXQED set.
- Reson. below 1 TeV, the situation is a bit better. Cross sections, an order of magnitude larger.
- Reson. of higher masses: maybe in collisions involving heavy ions. Pb-Pb: enhanced by a factor $(Z = 82)^2$, lost to a factor 2000 smaller luminosity than in pp collisions with the current LHC; perhaps p-Pb is optimal.
- Proposed luminosity of the CLIC collider, $\sim 650 \text{ fbarn}^1/\text{yr}$; our resonance σ , 10^3 fbarn ; only a couple of events per year. While CLIC may be apt for exploring vector resonances that couple in an s-wave to e^+e^- , it will fall short in luminosity for scalar or tensor resonances in $\gamma\gamma$ physics.